Parton Densities and DGLAP Evolution

Manuel Morales

April 26, 2020

Abstract

We study the parton model and how the parton distributions functions change with the scale at which we probe a composite system, like the proton. We see that this evolution is described by the DGLAP equations, which we implemented at leading order (LO). These equations can be solved by diagonalizing a coefficient matrix through a change of variables and the use of the Mellin transform and its inverse. We take as input the PDFs of [1] at $Q^2 = 1\ (GeV)^2$ and reproduce their result up to a 0.1% difference. We see that the PDFs deplete at higher x values, the relative contribution of quarks and gluons to the total momentum of the proton change, and also heavier flavours of quarks emerge from gluon splitting. We briefly discuss the limitations of LO analysis and how the inclusion of higher order corrections improve the results for the evolution of the PDFs.

1 Introduction

In this document we will discuss parton densities and the DGLAP evolution equation. These concepts are of fundamental importance to describe interactions between particles when we are working with hadrons, like in the Large Hadron Collider (LHC). They are necessary because the measurable quantities that we can obtain from collisions, like cross sections and decay rates, have encoded the influence the parton density functions.

Partons are the elementary constituents of hadrons, like quarks and gluons. The parton density function (PDF) of a given flavour of quark, antiquark or gluon $f_i(x)$ it is related to the probability that we find a parton of this type carrying a fraction x of the total momentum of the proton.

PDFs change when we vary the probing energy of the process we are interested in. This change in the PDFs can be described by the Dokshitzer-Gribov-Lipatov-Altarelli-Parisi (DGLAP) equations. If we know our parton distributions at a given scale, we can make them evolve using these equations to the energy values we need. This set of equations can be difficult to solve, so in order to work with them we will have to use the so-called Mellin transform and inverse Mellin transform of the distributions.

We will see how the distributions change with the probing scale, and how the contributions to the proton total momentum coming from quarks and gluons are transformed. We will also see how heavier flavour of quarks emerge inside the proton.

We will briefly discuss the inclusion of higher order corrections to our equations and how these give much more accurate results. These will extend our analysis and provide a better understanding of the underlying theory.

2 Deep inelastic scattering

Let us begin our discussion with a bit of history. Until the first half of the 20th century it was thought that protons were elementary particles, just like electrons. If that had been the case, then we would have been able to calculate, for example, the cross section for an $e^- p$ scattering using the standard QED Feynman rules.

We know now that the proton is not an elementary particle. Its gyromagnetic factor (the ratio between its magnetic moment and spin) it was proved to be $g_p \approx 5.59$, while it was known that for elementary particles this had to be $g_{\text{elem}} = 2$. It was shown experimentally that this parametrization did not give a good result, as it is presented in figure 1.

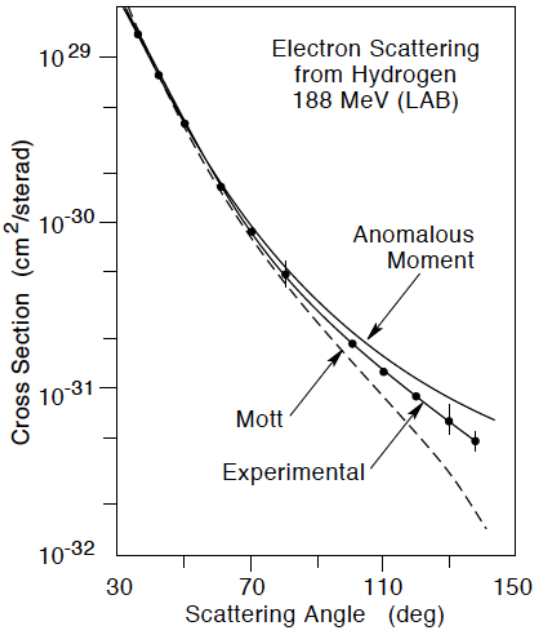

Figure 1: Experimental and theoretical model of the cross section of an $e^- p$ scattering at different angles. From [2].

Something had to be changed in the parametrization of the matrix element associated to this process. Let us start from an interaction between two real elementary particles, like in the

case of an $e^-\mu^n$ scattering. It can be shown using the Feynman rules for QED that the square of the matrix element for this process (averaged over all possible initial spin distributions and added on the final states) is given by

$$\overline{|M|^2} = \frac{e^4}{q^4} L^{\mu\nu}(e^-) L_{\mu\nu}(\mu^-), \tag{1}$$

where e is the charge of the electron and muon, q is the momentum of the photon exchanged, and $L^\mu\nu$ is the leptonic tensor of each particle. After integration on phase space this matrix element gives a good description of this process. To describe an e^-p, like in figure 2, scattering we can promote $L^{\mu\nu} \to W^{\mu\nu}$, where $W^{\mu\nu}$ is the hadronic tensor.

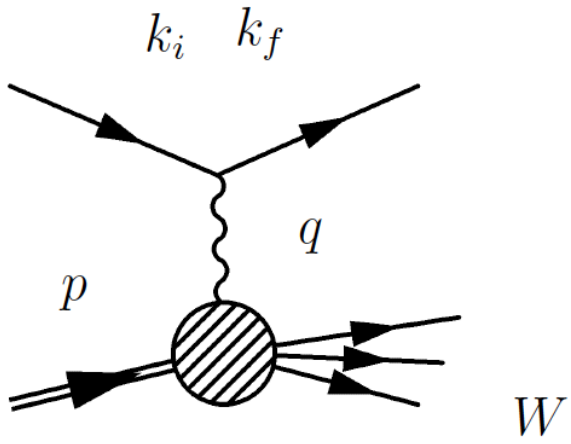

Figure 2: e^-p scattering. From [2].

The hadronic tensor can be decomposed in the most general case by all the symmetric rank-2 Lorentz structures of the scattering. These are the metric $g_{\mu\nu}$, the momentum of the incoming proton p^μ, and the momentum of the photon q^μ. In the most general case the hadronic tensor can be written as

$$W^{\mu\nu} = -M^2 W_1 g^{\mu\nu} + W_2 p^\mu p^\nu + W_3 q^\mu q^\nu + W_4 (p^\mu q^\nu + q^\mu p^\nu).$$

Charge conservation implies that the hadronic tensor must fulfill $q_\mu W^{\mu\nu} = 0$. This allows us to write it in its minimal form (2)

$$W_p^{\mu\nu} = W_1 \left(-g^{\mu\nu} + \frac{q^\mu q^\nu}{q^2} \right) + \frac{W_2}{M^2} \left(p^\mu - \frac{p\cdot q}{q^2} q^\mu \right) \left(p^\nu - \frac{p\cdot q}{q^2} q^\nu \right). \tag{2}$$

The coefficients $W_1(x, Q^2)$ and $W_2(x, Q^2)$, where $x = Q^2/(2p\cdot q)$ and $Q^2 \equiv -q^2$, are called structure functions. It can be shown that

$$L_{\mu\nu}(e^-) W^{\mu\nu}(p) = 4EE_f \left(W_2(Q^2, \nu) \cos^2 \frac{\theta}{2} + W_1(Q^2, \nu) \sin^2 \frac{\theta}{2} \right). \tag{3}$$

If we use (3) instead of the contraction of the two leptonic tensors of (1) we can see that the cross section of the $e^- p$ scattering depends on these structure functions. They are measurable quantities, and it is important that we understand how they can be calculated in order to study the interactions between the particles we are probing. In what follows, and following the commonly used notation in the literature, we will define

$$\begin{aligned} F_1(x, q^2) &\equiv M W_1(x, Q^2), \\ F_2(x, Q^2) &\equiv \frac{Q^2}{2Mx} W_2(x, Q^2). \end{aligned} \tag{4}$$

These two functions are also commonly named structure functions. We will see how these functions can be calculated in the next chapters.

3 The parton model

We saw the the proton is not at elementary particle but a composite system. If we probe the proton at shorter wavelength we should see its elementary constituents, the so-called partons,like quarks and gluons for example. Since we know that the wavelength of the photon exchanged between the electron and the proton satisfies $\lambda \sim 1/\sqrt{Q^2}$, at high Q^2 we should have a resolution inside the proton for shorter distances.

Let us consider that a parton carries a fraction x of the total momentum of the proton. The photon can interact with any of the partons, so in order to get the total cross section of the scattering we will have to sum up over all i partons of the proton. This is a QED cross section, so these sums will have to be weighted by the charge of parton. This is shown schematically in figure 3.

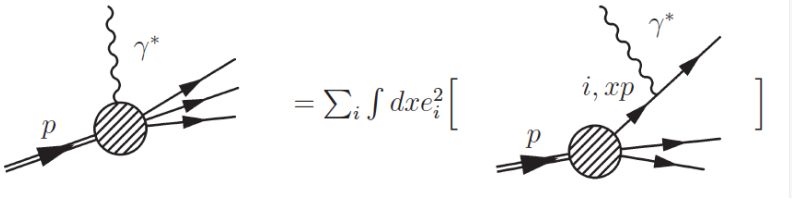

Figure 3: Inclusion of the individual partonic processes in the total cross section. From [2].

The photon can interact with any of the i quarks of the proton. The interacting quark can carry a fraction x of the total momentum of the proton with a probability described by a function $f_i(x, Q^2)$, which we will discuss more in detail in the next section. The total cross section of this process involves of course integrating the whole probability function and adding up the interaction with all of the i quarks. It is given by

$$\sigma = \int_0^1 dx \sum_i f_i(x, Q^2) \hat{\sigma}_i(x), \tag{5}$$

where $\hat{\sigma}_i(x)$ is the so-called hard cross section with takes into account the parton-photon interaction. We see that σ is described by two parts: the hard cross section and a contribution from the probability function. We say that σ has been factorized. Later we will discuss this factorization in detail, but it is related to a separation of scales that absorbs a possible gluon emission with very low transverse momentum into the probability functions.

For now we neglect QCD interactions. The structure functions (4) then can be written as

$$\begin{aligned} F_1(x,q^2) &= \frac{1}{2}\sum_i e_i^2 f_i(x), \\ \frac{F_2(x,Q^2)}{x} &= \sum_i .e_i^2 f_i(x), \end{aligned} \tag{6}$$

where $f_i(x)$ is the so-called parton distribution function of the type i quark.

4 Parton distribution functions

The parton distribution function (PDF) of the type i parton is denoted $f_i(x)$, and it can be understood as the probability that the photon interacts with a parton this carrying a fraction x of the total momentum of the proton. From now on we will commonly use the PDFs of the quarks, that we will denote $f_q(x,Q^2) = q(x,Q^2)$ and the gluons, denoted as $f_g(x,Q^2) = g(x,Q^2)$. It is useful to retain some schematic interpretations of quantities related to these PDFs. Let us consider, at a given probing scale Q^2, the PDF of the up quark $u(x,Q^2)$. We see that

- $u(x,Q^2)$: PDF of the up quarks.
- $u(x,Q^2)dx$: number of up quarks carrying a momentum fraction between x and $x+dx$ of the total momentum of the proton.
- $\int_0^1 xu(x,Q^2)dx$: fraction of the total momentum of the proton carried by up quarks.

The PDFs must satisfy certain conditions. In order for the proton to carry all its momentum, they must satisfy the so-called momentum sum rule

$$\sum_i \int_0^1 x f_i(x,Q^2)dx = 1, \tag{7}$$

where i runs over all partons.

The proton contains two up valence quarks and one down valence quark. However, due to pair splitting from gluons, the total number of up and down quarks can be potentially very big. To take this into account we define the valence distributions for the quarks as $f_{q_V}(x,Q^2) = f_q(x,Q^2) - f_{\bar{q}}(x,Q^2)$. These valence distributions must satisfy the so-called number sum rules, that for a proton are translated into

$$\int_0^1 u_V(x,Q^2)dx = 2,$$
$$\int_0^1 d_V(x,Q^2)dx = 1. \tag{8}$$

The momentum and number sum rules must be satisfied at any scale Q^2. These becomes an important feature to check when we calculate the evolution of the PDFs between different scales.
We will see that the relative contribution to the total momentum of the proton by the different partons change with the scale. At $Q = 1\ GeV$ we have that the quark and gluon contributions are

$$\sum_{i=q,\bar{q}} \int_0^1 x f_i(x)dx \approx 0.64,$$
$$\int_0^1 xg(x)dx \approx 0.36. \tag{9}$$

We see that gluons carry a considerable fraction of the momentum of the proton.

So far we have only addressed the QED part of the interactions. However, we must also include the QCD contributions. These involve interactions among quarks and gluons, as it is shown for example in figure 4. This process is of the kind $qg \to q\gamma^*$ and its cross section will be denoted $\hat{\sigma}$. The interacting parton carries a momentum $p_i = \xi P$, where P is the momentum of the proton. After the emission of the gluon the quark is left with a momentum $z\xi P \equiv xP$.

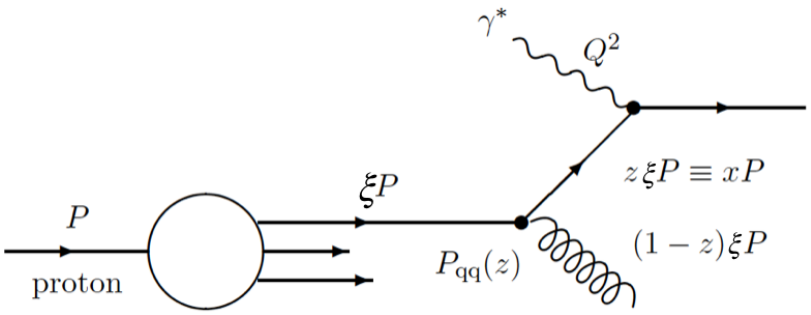

Figure 4: Parton-photon interaction with the emission of a gluon. From [4].

It can be proved that for small scattering angles in the center of mass frame

$$\frac{d\hat{\sigma}}{dk_T^2} = e_i^2 \hat{\sigma}_0 \frac{1}{k_T^2} \frac{\alpha_S}{2\pi} P_{qq}(z), \tag{10}$$

where k_T is the transverse momentum of the gluon, e_i is the fractional charge of the quark in units of the electron charge, $z = \frac{Q^2}{2p_i \cdot q} = \frac{x}{\xi}$ and

$$\hat{\sigma_0} = \frac{4\pi\alpha e_q^2}{\hat{s}}$$

is the Born cross section. In addition

$$P_{qq}(z) = C_F \frac{1+z^2}{1-z} \tag{11}$$

is the splitting function of the process. It is related to the probability for a quark to radiate a gluon and end up with a fraction z of its initial momentum. $C_F = 4/3$ is the well known color factor of this QCD vertex. Let us note that the cross section (10) exhibits two kinds of divergences. If $k_T \to 0$ we have a collinear divergence and if $z \to 1$ we see a soft gluon divergence (that will be regularized later). We will discuss this briefly.

If we want to get the inclusive cross section we must integrate over all the possible values of transverse momenta

$$\frac{\hat{\sigma}}{\sigma_0} \approx \frac{\alpha_S}{2\pi} P_{qq}(z) \int_{\mu^2}^{Q^2} \frac{dk_T^2}{k_T^2} = \frac{\alpha_S}{2\pi} P_{qq}(z) \log\left(\frac{Q^2}{\mu^2}\right), \tag{12}$$

where we have introduced an IR cutoff μ^2. This modifies the structure functions in (6) and we are left with

$$\frac{F_2(x,Q^2)}{x} = \sum_q \int_x^1 \frac{d\xi}{\xi} q(\xi) e_q^2 \left(\delta(1-x/\xi) + \frac{\alpha_S}{2\pi} P_{qq}(x/\xi) \log\frac{Q^2}{\mu^2}\right). \tag{13}$$

With the QCD correction a logarithmic dependence on the probing scale Q^2 has been introduced (note that without QCD we recover our original definition by integrating the delta function). We know that the structure functions are measurable quantities, and in the right hand side of (13) we can have an IR cutoff arbitrarily small, which would make the cross sections diverge. This inconsistency makes us redefine the PDFs up to a factorization scale

$$q(x,\mu_F^2) = q(x) + \frac{\alpha_S}{2\pi} \int_x^1 \frac{d\xi}{\xi} q(\xi) P_{qq}(x/\xi) \log\left(\frac{\mu_F^2}{\mu^2}\right), \tag{14}$$

where $q(x,\mu_F^2)$ is a physical PDF and $q(x)$ is the bare distribution. By doing this we are implying that any gluon emission with transverse momentum between μ and μ_F is absorbed in the integral of (14). Replacing the bare distribution in (13) we obtain

$$\frac{F_2(x,Q^2)}{x} = \sum_q \int_x^1 \frac{d\xi}{\xi} q(\xi) e_q^2 \left(\delta(1-x/\xi) + \frac{\alpha_S}{2\pi} P_{qq}(x/\xi) \log\frac{Q^2}{\mu_F^2}\right). \tag{15}$$

We fix our factorization scale $\mu_F^2 = Q^2$ to recover he original definitions in (6).

5 DGLAP evolution equations

So far we have dealt with how to calculate the structure functions at a fixed probing scale. Now we address the problem on how to the PDFs, and therefore the structure functions, evolve when we evolve in Q^2. The Q^2 dependence of the PDFs can be seen clearly from (14). We obtain

$$\frac{\partial q(x,Q^2)}{\partial \log(Q^2)} = \frac{\alpha_S}{2\pi}\int_x^1 \frac{d\xi}{\xi} q(\xi,Q^2) P_{qq}(x/\xi). \tag{16}$$

Now we need to expand our analysis. We have dealt only with the process of gluon emission from a quark, but there are other splitting contributions that affect the PDFs, which are shown in fig 5.

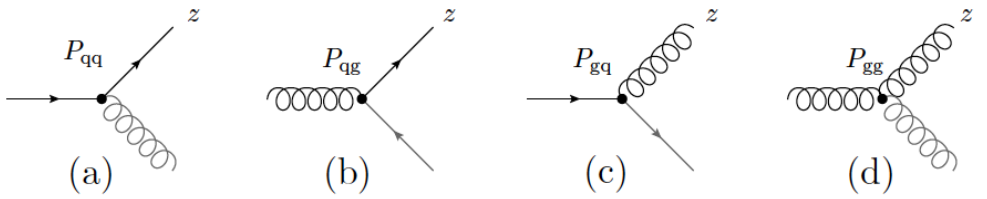

Figure 5: Splitting contributions. From [4].

As it is shown in detail in [5], conservation of the quark number allows us to regularize the $P_q q(z)$ splitting functions for soft gluon emission, giving

$$P_{qq}(z) = C_F\left(\frac{1+z^2}{(1-z)_+} + \frac{3}{2}\delta(1-z)\right), \tag{17}$$

where the '+' prescription is defined such that

$$\int_0^1 dz \frac{f(z)}{(1-z)_+} = \int_0^1 dz \frac{f(z)-f(1)}{1-z}.$$

The other splitting functions are given by

$$P_{gq}(z) = C_F\left(\frac{1+(1-z)^2}{z}\right), \tag{18}$$

$$P_{qg}(z) = T_F(z^2+(1-z)^2), \tag{19}$$

$$P_{gg}(z) = 2C_A\left(\frac{z}{(1-z)_+} + \frac{1-z}{z}\right) + \left(\frac{11C_A}{6} - \frac{3}{2}T_F n_f\right)\delta(1-z), \tag{20}$$

where $T_F = 1/2$ and $C_A = 3$ are the associated color factors of the given process. Together with this set of splitting functions, the PDFs satisfy the Dokshitzer-Gribov-Lipatov-Altarelli-Parisi (DGLAP) equations

$$\frac{\partial}{\partial \log(Q^2)}\begin{pmatrix} q(x,Q^2) \\ g(x,Q^2)\end{pmatrix} = \frac{\alpha_S(Q^2)}{2\pi}\int_x^1 \frac{dz}{z}\begin{pmatrix} P_{qq}(z) & P_{qg}(z) \\ P_{gq}(z) & P_{gg}(z)\end{pmatrix}\begin{pmatrix} q\left(\frac{x}{z},Q^2\right) \\ g\left(\frac{x}{z},Q^2\right),\end{pmatrix} \tag{21}$$

which is a system of $(2n_f + 1)$ coupled integro-differential equations, since we include the quark, antiquark, and gluons distributions of all possible active flavours n_f.

The system (21) can be very difficult to solve. A first step to make it more manipulable is to introduce a change of variables for valence, flavour and singlet quark PDFs, defined as

$$\begin{aligned} q_i^V &= q_i - \bar{q}_i, \\ q_i^F &= \sum_{k=1}^{i-1} (q_k + \bar{q}_k - q_i - \bar{q}_i), \\ q^S &= \sum_{k=1}^{n_f} (q_k + \bar{q}_k). \end{aligned} \tag{22}$$

We use n_f valence distributions, $(n_f - 1)$ flavour distributions and the singlet to recover the $2n_f$ quark PDFs. Gluons remain unchanged. This allows us to partially diagonalize (21) and obtain

$$\begin{aligned} \frac{\partial q_i^V(x,Q^2)}{\partial \log(Q^2)} &= \frac{\alpha_S(Q^2)}{2\pi} \int_x^1 P_{qq}(\xi) q_i^V(x/\xi, Q^2) \frac{d\xi}{\xi}, \\ \frac{\partial q_i^F(x,Q^2)}{\partial \log(Q^2)} &= \frac{\alpha_S(Q^2)}{2\pi} \int_x^1 P_{qq}(\xi) q_i^F(x/\xi, Q^2) \frac{d\xi}{\xi}, \end{aligned} \tag{23}$$

for the valence and flavour non-singlets distributions. These do not couple to the gluon PDF. The quark singlet distribution does couple to gluons and their evolution is described by

$$\frac{\partial}{\partial \log(Q^2)} \begin{pmatrix} q^S(x,Q^2) \\ g(x,Q^2) \end{pmatrix} = \frac{\alpha_S(Q^2)}{2\pi} \int_x^1 \frac{dz}{z} \begin{pmatrix} P_{qq}(z) & 2n_f P_{qg}(z) \\ P_{gq}(z) & P_{gg}(z) la \end{pmatrix} \begin{pmatrix} q^S\left(\frac{x}{z}, Q^2\right) \\ g\left(\frac{x}{z}, Q^2\right). \end{pmatrix} \tag{24}$$

The $2n_f$ factor in the matrix of splitting functions comes from the fact that a gluon can resolve into a quark-antiquark pair (which in the singlet distribution are added up) of all n_f flavours involved.

We have been able to decouple the evolution of some of the PDFs, but we still have to solve one coupled integro-differential system, which is still pretty difficult. However, there is a mathematical resource that we can use to make the evolution equations simpler: the Mellin transform.

6 Mellin and inverse Mellin transforms

The Mellin transform of a function $f_i(x)$ is defined as

$$\mathcal{M}[f(x)](j) = f_i(j) = \int_0^1 x^j f_i(x) \frac{dx}{x} = \int_0^1 x^{j-1} f_i(x) dx. \tag{25}$$

The Mellin transform is a linear operator that has many useful properties involving derivatives of the transformed function, scalings, and translations, to mention a few. However,

there is one property that is of particular importance for the DGLAP evolution. Let us define the convolution

$$(f \otimes g)(x) \equiv \int_x^1 f(\xi) g\left(\frac{x}{\xi}\right) \frac{d\xi}{\xi}.$$

The Mellin transform satisfies

$$M[(f \otimes g)(x)](n) = M[f(x)](n) \cdot M[g(x)](n), \tag{26}$$

meaning that the Mellin transform of a convolution of functions is just the ordinary product of the individual transforms. These means that if we take the Mellin transform in (23) and (24) we can get rid of the integration and solve only a differential equation. Equation (26) can be proved by noting that

$$\begin{aligned} M[(f \otimes g)(x)](n) &= \int_0^1 \int_x^1 x^{n-1} f(\xi) g(x/\xi) \frac{d\xi}{\xi} dx \\ &= \int_0^1 \int_0^\xi x^{n-1} f(\xi) g(x/\xi) \frac{d\xi}{\xi} dx, \end{aligned}$$

where we have changed the limits of integration given that $0 < x < \xi < 1$. Defining $z = x/\xi \Rightarrow dz = dx/\xi$, we have

$$\begin{aligned} M[(f \otimes g)(x)](n) &= \int_0^1 \int_0^\xi \left(\frac{x}{\xi}\right)^{n-1} \xi^{n-1} f(\xi) g(x/\xi) \frac{d\xi}{\xi} dx \\ &= \int_0^1 \int_0^1 z^{n-1} \xi^{n-1} f(\xi) g(z) dz d\xi \\ &= \int_0^1 \xi^{n-1} f(\xi) d\xi \cdot \int_0^1 z^{n-1} g(z) dz \\ &= M[f(x)](n) \cdot M[g(x)](n). \end{aligned}$$

With this convolution property we get rid of the aforementioned integrals. If we apply the Mellin transform to the equations (23) and (24) the DGLAP equations for the decoupled PDFs become

$$\begin{aligned} \frac{\partial q_i^V(n, Q^2)}{\partial \log(Q^2)} &= \frac{\alpha_S(Q^2)}{2\pi} P_{qq}(n)\ q_i^V(n, Q^2), \\ \frac{\partial q_i^F(n, Q^2)}{\partial \log(Q^2)} &= \frac{\alpha_S(Q^2)}{2\pi} P_{qq}(n)\ q_i^F(n, Q^2), \end{aligned} \tag{27}$$

while for the coupled PDF we are left with

$$\frac{\partial}{\partial \log(Q^2)} \begin{pmatrix} q^S(n, Q^2) \\ g(n, Q^2) \end{pmatrix} = \frac{\alpha_S(Q^2)}{2\pi} \begin{pmatrix} P_{qq}(n) & 2n_f P_{qg}(n) \\ P_{gq}(n) & P_{gg}(n) \end{pmatrix} \begin{pmatrix} q^S(n, Q^2) \\ g(n, Q^2) \end{pmatrix}, \tag{28}$$

where the Mellin transform of the splitting functions (at leading order) are given by [6]:

$$
\begin{aligned}
P_{qq}^{(0)}(n) &= C_F \left[-\frac{1}{2} + \frac{1}{n(n+1)} - 2\sum_{k=0}^{n} \frac{1}{k} \right], \\
P_{qg}^{(0)}(n) &= T_R \left[\frac{2+n+n^2}{n(n+1)(n+2)} \right]], \\
P_{gq}^{(0)}(n) &= C_F \left[\frac{2+n+n^2}{n(n^2-1)} \right]], \\
P_{gg}^{(0)}(n) &= 2C_A \left[-\frac{1}{12} + \frac{1}{n(n-1)} + \frac{1}{(n+1)(n+2)} - \sum_{k=0}^{n} \frac{1}{k} \right] \frac{2}{3} n_f T_R.
\end{aligned}
$$

The PDFs described by (27) can be integrated directly by using the RG equation for the strong coupling α_S at LO

$$
\frac{\partial a_S}{\partial \log(Q^2)} = -\alpha_S \left(\beta_0 \frac{\alpha_S}{4\pi} \right), \tag{29}
$$

where $\beta_0 = 11/3 - 2/3 n_f$. We are left with

$$
\begin{aligned}
q_i^V(n, Q^2) &= q_i^V(n, Q_0^2) \left(\frac{\alpha_S(Q^2)}{\alpha_S(Q_0^2)} \right)^{-\frac{2}{\beta_0} P_{qq}(n)}, \\
q_i^F(n, Q^2) &= q_i^F(n, Q_0^2) \left(\frac{\alpha_S(Q^2)}{\alpha_S(Q_0^2)} \right)^{-\frac{2}{\beta_0} P_{qq}(n)},
\end{aligned} \tag{30}
$$

where we have integrated between between an initial reference scale Q_0^2 and a final one Q^2. The coupled system (28) can be solved by using computational softwares (like Mathematica, for example) that diagonalize the coefficient matrix.

To return to the x domain and recover the actual PDFs we use the inverse Mellin transform, defined as

$$
f_i(x) = \frac{1}{2\pi i} \int_C x^{-n} f_i(n) dn, \tag{31}
$$

where C is a curve than runs parallel to the imaginary axis and it is located to the right of all the singularities of $f_i(n)$. The inverse Mellin transform can be calculated numerically and, due to the Cauchy's theorem, we can deform the integration contour for our convenience, as it is shown in fig 6.

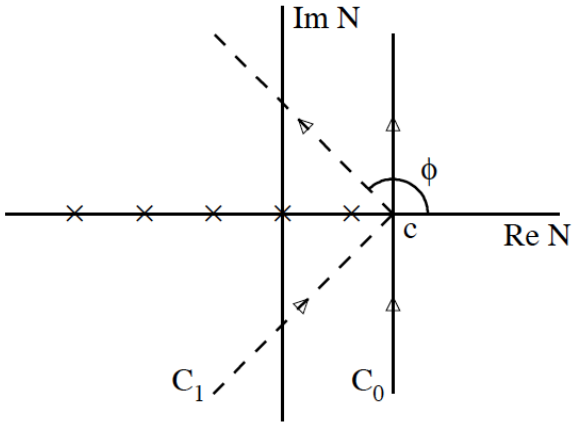

Figure 6: Two integration contours C_0 and C_1 with which we can calculate the inverse Mellin transform. From [3].

It is usually more convenient to use a contour similar to C_1, with an angle $\phi > \pi/2$. This gives us an exponential damping due to the factor x^{-n} in (31) that makes the integral converge faster.

7 The model and its evolution

We posses now all the theoretical framework to study the evolution of PDFs. We will base our study on [1], the MSTW collaboration. Our aim is to see how the PDFs for quarks, antiquarks, and gluons change when we make them evolve from an initial scale $Q_0^2 = 1\ (GeV)^2$ to a final scale $Q_f^2 = 10000\ (GeV)^2$.

We will take as input the PDFs at the initial scale Q_0^2 following the next functional ansatz:

$$xu_v(x,Q_0^2) = A_u x^{\eta_1}(1-x)^{\eta_2}(1+\epsilon_u\sqrt{x}+\gamma_u x), \tag{32}$$
$$xd_v(x,Q_0^2) = A_d x^{\eta_3}(1-x)^{\eta_4}(1+\epsilon_d\sqrt{x}+\gamma_d x), \tag{33}$$
$$xS(x,Q_0^2) = A_S x^{\delta_S}(1-x)^{\eta_S}(1+\epsilon_S\sqrt{x}+\gamma_S x), \tag{34}$$
$$x\Delta(x,Q_0^2) = A_\Delta x^{\eta_\Delta}(1-x)^{\eta_S+2}(1+\gamma_\Delta x+\delta_\Delta x^2), \tag{35}$$
$$xg(x,Q_0^2) = A_g x^{\delta_g}(1-x)^{\eta_g}(1+\epsilon_g\sqrt{x}+\gamma_g x), \tag{36}$$
$$x(s+\bar{s})(x,Q_0^2) = A_+ x^{\delta_S}(1-x)^{\eta_+}(1+\epsilon_S\sqrt{x}+\gamma_S x), \tag{37}$$
$$x(s-\bar{s})(x,Q_0^2) = A_- x^{\delta_-}(1-x)^{\eta_-}(1-x/x^0), \tag{38}$$

where $\Delta \equiv \bar{d}-\bar{u}$, $q_v \equiv q-\bar{q}$ and the quark sea contribution $S \equiv 2(\bar{u}+\bar{d})+s+\bar{s}$. These functional forms can describe properly the behaviour of the PDFs for both $x \approx 0$ and $x \approx 1$, and they are also simple functions to apply the Mellin transform and its inverse on.

As we discussed in earlier sections, the PDFs must satisfy the sum rules

$$\int_0^1 dx\ u_v(x, Q_0^2) = 2, \tag{39}$$

$$\int_0^1 dx\ d_v(x, Q_0^2) = 1, \tag{40}$$

$$\int_0^1 dx\ s_v(x, Q_0^2) = 0, \tag{41}$$

and the momentum sum rules, which with our definitions it is translated into

$$\int_0^1 dx x \left[u_v(x, Q_0^2) + d_v(x, Q_0^2) + S(x, Q_0^2) + g(x, Q_0^2)\right] = 1. \tag{42}$$

The parameters for the PDFs were found by the MSTW collaboration. The nominal values at leading order are shown in table 1. The details on the uncertainties of these parameters can be found in the original paper.

Parameter	Value at LO	Parameter	Value at LO
$\alpha_S(Q_0^2)$	0.68183	γ_S	16.865
$\alpha_S(M_Z^2)$	0.13939	A_Δ	8.9413
A_u	1.4335	η_Δ	1.8760
η_1	0.45232	γ_Δ	8.4703
η_2	3.0409	δ_Δ	-36.507
ϵ_u	-2.3737	A_g	0.0012216
γ_u	8.9924	δ_g	-0.83657
A_d	5.0903	η_g	2.3882
η_3	0.71978	ϵ_g	-38.997
$\eta_4 - \eta_2$	2.0835	γ_g	1445.5
ϵ_d	-4.3654	A_+	0.10302
γ_d	7.4730	η_+	13.242
A_S	0.59964	A_-	-0.011523
δ_S	-0.16276	δ_-	0.200
η_S	8.8801	η_-	10.285
ϵ_S	-2.9012	x_0	0.017414

Table 1: Nominal values of the PDF parameters at LO.

Using these values we have a concrete functional form for all the PDFs and now we can make them evolve using the DGLAP equation.

When we are moving up in the probing scale from Q_0^2 to Q_f^2 the number of active flavours n_f is modified. This changes the functional form of the strong coupling due to the dependence of the β_0 factor in (29). The masses of the quarks in the $\overline{MS}$ scheme are known to be $m_u, m_d \sim 1\ MeV$, $m_s \sim 100\ MeV$, $m_c \sim 1.2\ GeV$ and $m_b \sim 4\ GeV$. These separates the evolution in three steps:

1. Evolution from $Q_0^2 \to m_c^2$, where $n_f = 3$.
2. Evolution from $m_c^2 \to m_b^2$, where $n_f = 4$.
3. Evolution from $m_b^2 \to Q_f^2$, where $n_f = 5$.

What we do is to take the Mellin transform of the initial distributions, make them evolve according to these three aforementioned steps in Mellin space, and then take the inverse Mellin transform at the final scale to recover the results in x- space.

8 Results

The evolution between scales of the u, $\bar{u}$, d, $\bar{d}$ and g PDFs is shown in figure 7. Our results match at a 0.1 % difference with the results of the MSTW collaboration, which can be found using their code and grids on https://mstwpdf.hepforge.org/.

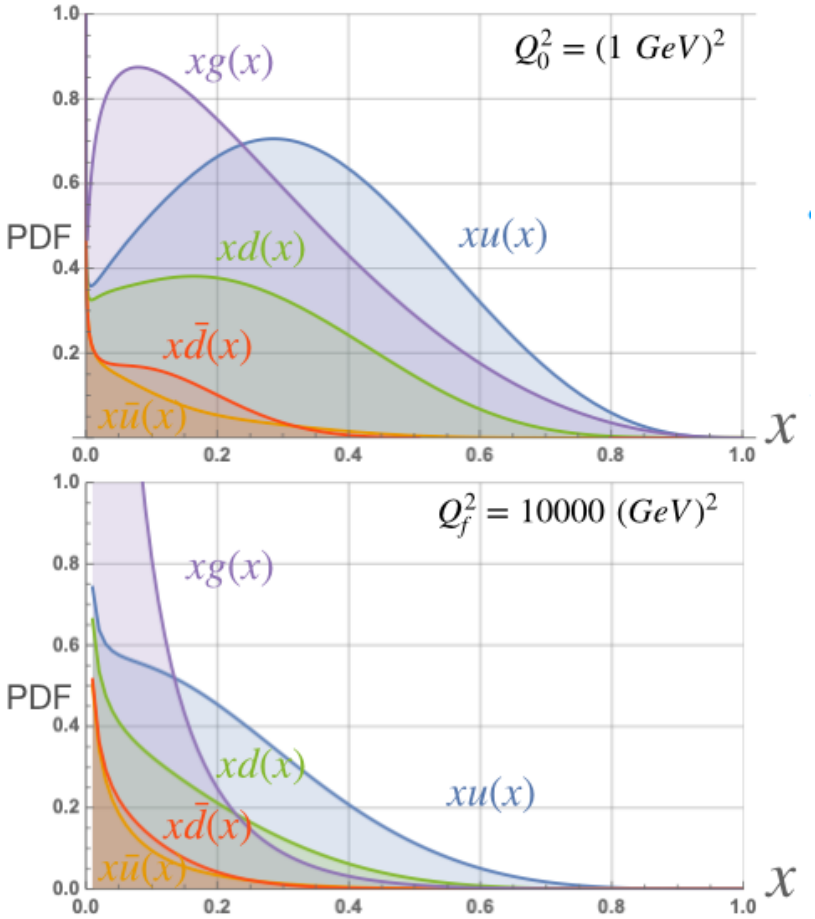

Figure 7: PDFs of the gluons and the two lightest flavours quarks and antiquarks at the initial and final scales.

We see that for higher Q^2 the PDFs deplete at higher x values. This comes from the fact that a high momentum transfer from the virtual photon to one of the quarks of the proton

leaves it with a lot of energy that can be radiated by gluon emission, which later can become quark-antiquark pairs. This implies that the total momentum of the proton is carried by a larger number of partons, with each one of them carrying a smaller fraction of the total momentum. This comes directly from the momentum sum rule.

This gluon emission also implies that, at higher Q^2, a bigger portion of the momentum of the proton is carried by them. At Q_0^2 they carry around 36 % of the momentum, while at Q_f^2 they carry around a 49 % of it. Naturally the quark contribution is reduced due to momentum conservation.

We also see that at higher Q^2 and small x the gluon PDF grows substantially. This is consonant with the fact that quarks can radiate a great number of low energy gluons. We already discussed the fact that even soft gluon emission is encoded in the PDFs, which explains the divergence when $x \to 0$.

We can also study the PDFs of the s, $\bar{s}$, c, $\bar{c}$, b and $\bar{b}$ quarks, which are shown in figure 8.

We see that only the distributions for the s and $\bar{s}$ quarks are active at $Q_0^2 = 1\ (GeV)^2$, while the other PDFs are strictly zero for all x. This comes from the fact that at this energy scale a gluon has not enough energy to resolve into a quark pair of c or b type, but we are above the mass threshold of the s quarks.

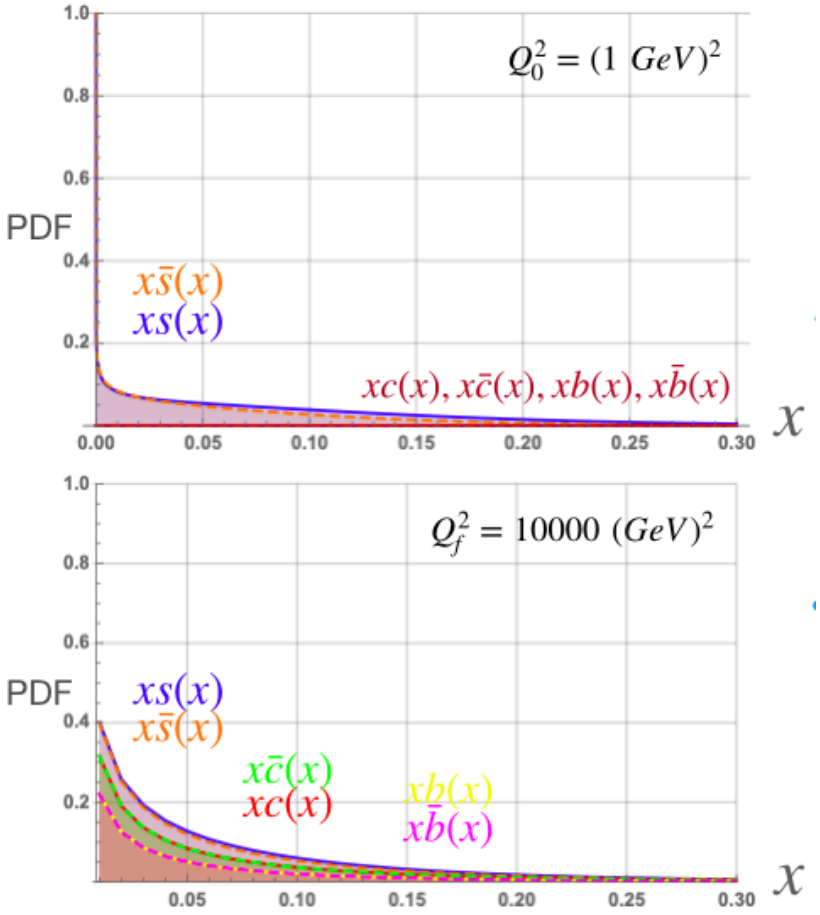

Figure 8: PDFs of the three heavier flavours of quarks and antiquarks at the initial and final scales.

At Q_f^2 we see that the PDF of the c and b type quarks are now active. Now we have gluon splitting that can resolve in the creation of pairs of these types. We have a greater number of quarks in the small x region. We see that all these distributions are the same for quark and antiquark pairs, which is natural since the proton does not posses any valence content for these flavours (unlike for the u and d quarks). The heavier a flavour is, the lower is its PDF. These comes from the fact that, although the energy scale is well above all the masses of the quarks involved (the difference in their PDFs is not that big), it is still slightly more expensive energetically to produce heavier flavours from gluon splitting.

9 Limitations of LO analysis

In this project we worked out the DGLAP evolution equations at LO. This simplifies the calculations, but it also comes with the price of having a greater uncertainty at the time of describing how the PDFs change with the probing scale, as it is shown in figure 9. At LO we see that the uncertainty on the PDFs of the gluon, for example, is of the order of 30%. This uncertainty is reduced to 5% and 2% at NLO and NNLO, respectively.

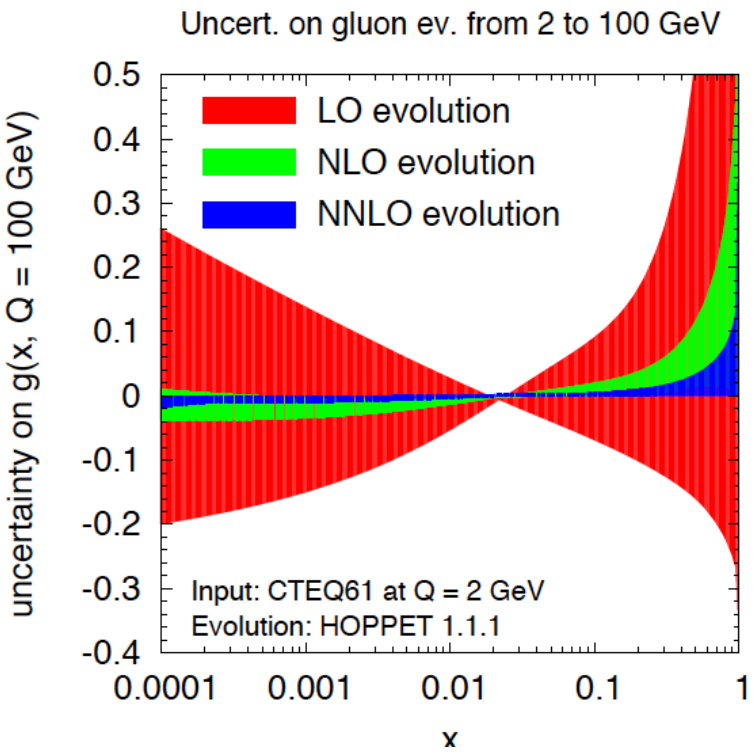

Figure 9: Inclusion of the individual partonic processes in the total cross section. From [7].

At higher orders the computations become harder. We cannot use the LO expression of the strong coupling (29), but instead we must use higher order terms of the beta function

$$\frac{\partial a_S}{\partial \log(Q^2)} = -\alpha_S \left(\beta_0 \frac{\alpha_S}{4\pi} + \beta_1 \left(\frac{\alpha_S}{4\pi} \right)^2 + ... \right). \tag{43}$$

For example, at NLO, we must retain two terms in the right hand side of (43). After some algebra it can be shown that

$$\frac{1}{a_S(Q^2)} = \frac{1}{a_S(Q_0^2)} + \beta_0 \ln\left(\frac{Q^2}{Q_0^2}\right) - b_1 \log\left(\frac{a_S(Q^2)[1 + b_1 a_S(Q_0^2)]}{a_S(Q_0^2)[1 + b_1 a_S(Q^2)]}\right),$$

where $b_1 = \beta_1/\beta_0$, and $\beta_1 = 102 - 38/3 n_f$. This equation does not even allow to obtain explicitly $\alpha_S(Q^2)$, but instead all we can get is an implicit relation for it. It can be solved numerically by using Runge-Kutta integration.

Additional difficulties arise also with respect to the splitting functions. Now we have even more splitting processes that are non vanishing in the DGLAP equation (21). Additionally, the at higher orders the splitting function for quark entries must be written in its most general way as

$$P_{q_i q_j}(z, \alpha_S(Q^2)) = \delta_{ij} P_{qq}^{(0)}(z) + \frac{\alpha_S(Q^2)}{2\pi} P_{qq}^{(1)}(z) + ...$$

This implies that, even after taking the Mellin transform of the DGLAP equation, we are left with a coupled system of differential equations with variable coefficients in the matrix,

while before they were constant with respect to the probing scale Q^2. Now it enters into the equation through its relation with the strong coupling.

10 Conclusions

In this project we have discussed PDFs and the DGLAP evolution equation, which describe how the PDFs evolve when we change the probing scale Q^2.

By introducing notions of DIS, we discussed the importance of the PDFs in the cross sections calculated from process regarding hadrons through their connection with the structure functions. Then we introduced the parton model, which tells us that at higher resolutions the interaction with the photon takes place with elementary constituents of the proton, the quarks. We introduced the PDFs to describe what is the probability that we find a parton carrying a given momentum fraction of the total proton, and defined the sum rules the PDFs must fulfill. We also found that the gluon contribution to the total momentum at the scales we worked is highly relevant. Afterwards, we included QCD corrections in our diagrams and presented the splitting functions, which are related to the probability that an original parton gives place to a final one with a given fractions of its initial momentum. We discussed how these QCD correction break the x scaling, and how infrared divergences made us redefine the PDFs using a factorization scale. The variation of the PDFs with respect to this scale, fixed to be equal to the probing scale, gave us the DGLAP evolution equations.

We included all the regularized splitting functions and deduced the most general DGLAP equation. By introducing valence, flavour, and singlet distributions we were able to partially diagonalize the system. In addition, the Mellin transform allowed us to transform an integral convolution of functions into an ordinary product, making these equations much easier to solve. We make the PDFs evolve in Mellin space and then recover the distributions in x space by applying the inverse Mellin transform using an integration contour that made the convergence optimal.

We took as an input the PDFs found by the MSTW collaboration [1] at a scale of $Q_0^2 = 1\ (GeV)^2$ and made them evolve to a final scale $Q_f^2 = 10000\ (GeV)^2$. We divided the evolution in different steps since the number of active flavour changed during the process, affecting the definition of the strong coupling. we found that the PDFs depleted at higher x values and the relative contribution of gluons to the total momentum of the proton increased. We also saw how the heavier flavour of quarks emerge inside the proton at higher probing energies.

There is still a lot to be done. We must extend the analysis to higher order corrections to reduce the uncertainty on the evolution of the PDFs to have a better understanding of this strongly coupled system that is the proton.

References

[1] A. D. Martin, W. J. Stirling, R. S. Thorne, G. Watt, *Parton distributions for the LHC*, 2009., https://arxiv.org/abs/0901.0002v3.

[2] V.Chiochia, G. Dissertori, T. Gehrmann, *Phenomenology of Particle Physics II*, ETH Zürich and the University of Zürich, 2010.

[3] A. Vogt, *Efficient evolution of unpolarized and polarized parton distributions with QCD-PEGASUS*, https://arxiv.org/abs/hep-ph/0408244.

[4] Michiel Botje, *Lecture Notes Particle Physics II*, Nikhef, Science Park, Amsterdam, 2013.

[5] Halzen F. and Martin A.,*Quarks and Leptons: An Introductory Course in Modern Particle Physics*, John Wiely and Sons, 1984.

[6] Ellis R. K. , Stirling W. J. and Webber B. R., *QCD and Collider Physics*, Cambridge Monographs in Particle Physics, Nuclear Physics and Cosmology.

[7] Salam G., *Lecture 2: Parton Distribution Functions*, European School of High-Energy Physics, 2009.